MNRAS 000, 1–6 (XXXX) Preprint 6 October 2015 Compiled using MNRAS LATEX style file v3.0

The sparkling Universe: the coherent motions of cosmic voids

Diego G. Lambas⋆, Marcelo Lares, Laura Ceccarelli, Andrés N. Ruiz, Dante J. Paz, Victoria E. Maldonado & Heliana E. Luparello

Instituto de Astronomía Teórica y Experimental (IATE), CONICET-UNC
Observatorio Astronómico, Universidad Nacional de Córdoba, Argentina.

Accepted XXX. Received XXX; in original form XXX

ABSTRACT

We compute the bulk motions of cosmic voids, using a ΛCDM numerical simulation considering the mean velocities of the dark matter inside the void itself and that of the haloes in the surrounding shell. We find coincident values of these two measures in the range $\sim$ 300-400 km s^{-1}, not far from the expected mean peculiar velocities of groups and galaxy clusters. When analysing the distribution of the pairwise relative velocities of voids, we find a remarkable bimodal behaviour consistent with an excess of both systematically approaching and receding voids. We determine that the origin of this bimodality resides in the void large scale environment, since once voids are classified into void-in-void (R–type) or void-in-cloud (S–type), R–types are found mutually receding away, while S–types approach each other. The magnitude of these systematic relative velocities account for more than 100 km s^{-1}, reaching large coherence lengths of up to 200 h^{-1} Mpc . We have used samples of voids from the Sloan Digital Sky Survey Data Release 7 (SDSS-DR7) and the peculiar velocity field inferred from linear theory, finding fully consistent results with the simulation predictions. Thus, their relative motion suggests a scenario of a sparkling Universe, with approaching and receding voids according to their local environment.

Key words: Cosmology: large scale structure of Universe – Cosmology: observations

1 INTRODUCTION

The distribution of galaxies at large scales reveals a complex structure where cosmic voids, underdense nearly spherical regions devoid of galaxies, arise as matter flows away from primordial underdense perturbations toward filaments and walls. New insights on the distribution and dynamics of these structures to unprecedented large cosmological scales, will be available by upcoming surveys such as HETDEX (Hill et al. 2008) or Euclid (Amendola et al. 2013). Since it is widely believed that voids are weakly clustered and have negligible velocities, their study is promising for the field of observational cosmology.

Although the large scale galaxy and mass distributions are dominated by filaments and walls, a larger fraction of the volume of the Universe is occupied by voids that can be used in several cosmological tests (Lavaux & Wandelt 2010; Bos et al. 2012), and galaxy evolution models(Ceccarelli et al. 2008; Ricciardelli et al. 2014). As the Universe evolves and galaxies flow away from voids, the supercluster-void network emerges (Frisch et al. 1995; Einasto et al. 1997, 2012). The global flows of mass associated with this clustering process are expected to be significant up to the scales of the largest structures, vanishing to a random component at larger scales. Cosmic bulk flows have been reported in the local Universe at scales of a few hundred Mpc, some of them challenging the ΛCDM model (Watkins et al. 2009; Lavaux et al. 2010; Feldman et al. 2010; Colin et al. 2011). and others in agreement with this structure formation scenario (Nusser et al. 2011; Branchini et al. 2012; Turnbull et al. 2012; Ma & Pan 2014; Hoffman et al. 2015). It is well known that voids are approximately in isotropic expansion, a direct consequence of their low density contrast in the central regions (van de Weygaert & Bertschinger 1996; Padilla et al. 2005; Ceccarelli et al. 2006). However, it has not been studied into detail the bulk velocity of the void region and that of the surrounding shell of galaxies, the main aim of this work.

2 VOID CATALOGUES

Cosmic voids can be identified both in simulations and in observational catalogues. We use a Voronoi tesselation technique to identify the lowest density regions, which serve as candidates for void search. We use a dark matter N-body simulation of 1024^3 particles in a comoving box of side 1000 h^{-1} Mpc in the standard ΛCDM scenario. We select cosmological parameters according to WMAP9 data (Hinshaw et al. 2013): $\Omega_M = 0.279$, $\Omega_\Lambda = 0.721$, $\Omega_b = 0.0462$, $h = 0.7$, $n = 0.972$ and $\sigma_8 = 0.821$. The initial conditions were generated using MUSIC (Hahn & Abel 2011) and the simulation was evolved to $z = 0$ with the public version of GADGET-2 (Springel 2005). Dark matter haloes were identified as bound structures using the ROCKSTAR code (Behroozi et al. 2013). The final catalogue consists of 3983265 haloes with at least 20 particles. To construct

⋆ e-mail: dgl@oac.unc.edu.ar

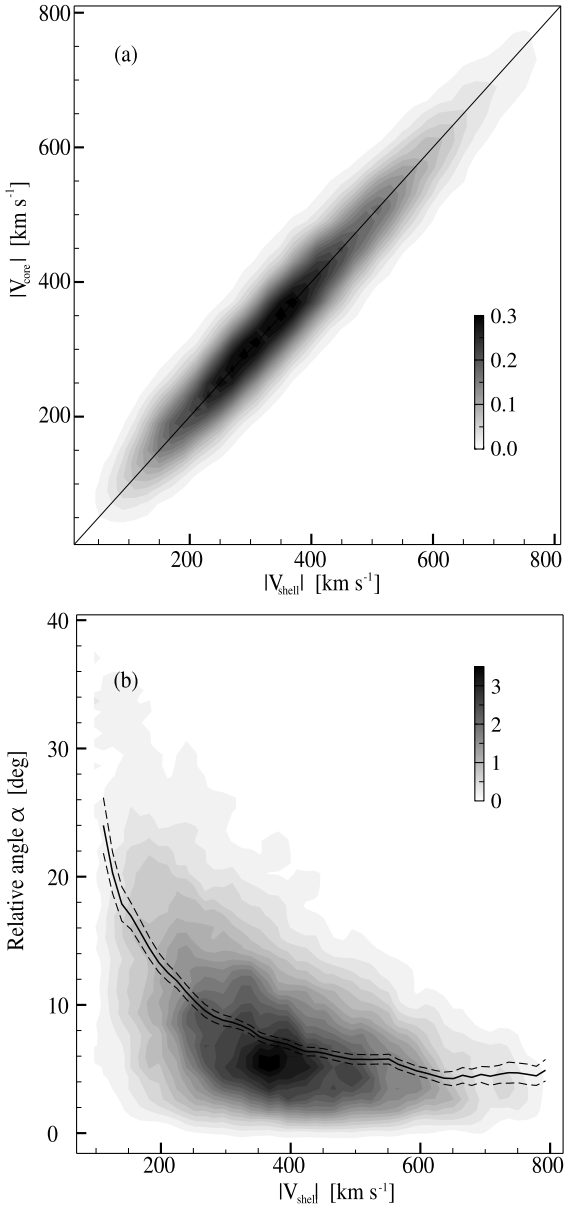

Figure 1. Bulk velocities of void shells and cores in the simulation. The shell velocity corresponds to the dark matter haloes mean velocity within $0.8 < r/R_{void} < 1.2$. Void core velocity corresponds to the mean of dark matter particles within $0.8\,R_{void}$. (a) Distribution function of void counts in $|V_{shell}|$, $|V_{core}|$ bins. Solid line shows the one-to-one relation, close to the linear fit results with slope 0.96. (b) Distribution function of void counts in bins of $|V_{shell}|$ and the relative angle α between shell and core bulk velocities. Solid and dashed lines correspond to the median and its standard error.

the void catalogues we followed the procedure described in Ruiz et al. (2015), which is a modified version of the procedures presented in Padilla et al. (2005) and Ceccarelli et al. (2006). The density estimation is performed using a Voronoi tessellation on the halo catalogue, where underdense cells are selected as void center candidates. We consider spheres centered in those positions and compute the integrated density contrast (namely $\Delta(r)$) at increasing values of radius, then selecting as void candidate the largest sphere satisfying the condition $\Delta(r) < -0.9$. After that, the center position is randomly tilted and the sphere is allowed to grow in order to recenter the void, so that a void of radius $R_{\rm void}$ is the largest sphere satisfying the underdense condition and not overlapping with any other underdense sphere. The final catalogue comprises 13430 voids in the simulation box with radii in the range 8–30 h^{-1} Mpc .

In a similar fashion, we identified voids in the observations using the Main Galaxy Sample of the Sloan Digital Sky Survey Data Release 7 (Abazajian et al. 2009). The spectroscopic catalogue comprises in this release 929555 galaxies with a limiting magnitude of $r \leqslant 17.77$. We adopted volume complete samples with a limiting redshift $z = 0.12$ and a maximum absolute magnitude in the $r-$band of $M_r = -20.3$. The limiting redshift of the sample is determined by the dilution of the sample of galaxies required to achieve statistically significant results. Moreover, the minimum number of particles for haloes used to identify voids in the simulation was chosen so that the number density of tracers in both cases are comparable. More details on the choice of parameters that affect the properties of the void sample are given in (Paz et al. 2013).

2.1 Linear velocity field in the SDSS

We have adopted the peculiar velocity field derived from linear theory by Wang et al. (2012). The method is described in detail in Wang et al. (2009). Briefly, these authors use groups of galaxies as tracers of dark matter halos and its cross correlation function with mass, in order to estimate the matter density field over the survey domain. The linear theory relation between mass overdensity and peculiar velocity is used to reconstruct the 3D velocity field. To test the accuracy of this method they use a mock catalogue that reproduces the main features of the SDSS-DR7 survey. The authors compare the actual three–dimensional velocities from the simulation box and the reconstructed velocity field in the mock catalogue. They show that reconstructed velocities are linearly correlated with actual velocities. By analysing this correlation as a function of the mock catalogue boundaries, they infer that the bias in the reconstruction is small in the inner region of the survey. The volume for which this field is reliably determined on this method is approximately two thirds of the total volume of the SDSS galaxy sample. Thus, we have considered 245 voids, ranging sizes between 5 and 23 h^{-1} Mpc , identified in the observational data restricted to this smaller region. In order to asses the effects of this procedure on the motion of void shells, we have compared the mean fully non–linear velocities of haloes within void shells in the simulation and the mean linearized velocities computed in the same shell volume. We find that the two vector are typically aligned within 15 degrees and with moduli differing less than 30%, showing that linear theory provides a suitable approximation to the actual void shell velocities.

3 VOID MOTIONS AND PAIRWISE VELOCITIES

3.1 Bulk velocities of void shells and cores in the simulation

In the simulation, we have computed the mean motions of mass (particles) in the central regions of voids ($r/R_{void} < 0.8$) as well as the mean motions of the haloes in the surrounding shells ($0.8 < r/R_{void} < 1.2$). The median values of velocity moduli and relative angle between the two void velocity measures are shown in Figure 1, indicating that either using particles or haloes, the motion of cosmic voids is not negligible at all. It can be noticed that the dark matter in the void inner region and the haloes in the surrounding shell, exhibit remarkably similar velocities, both in magnitude and

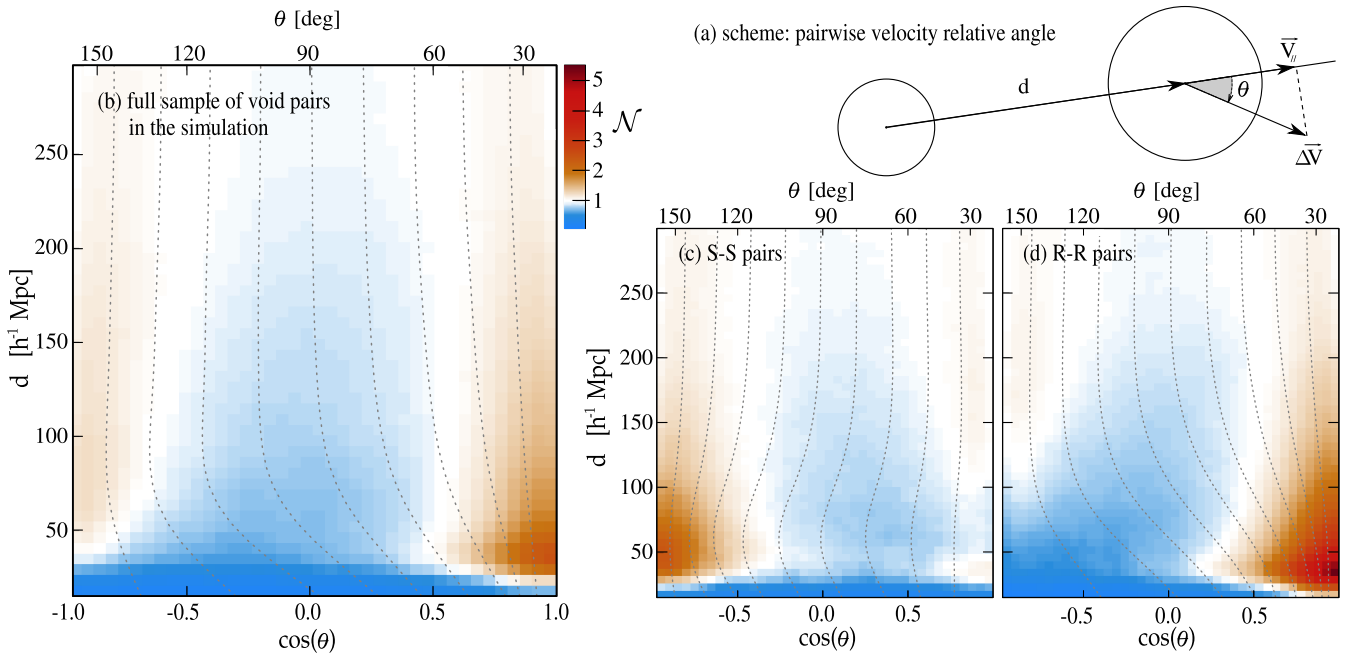

Figure 2. Coherence and bimodality of cosmic void relative motions. We show $\mathcal{N}$, the number counts of void pairs as a function of cos(θ) and separation, normalized to the expected number for a uniform distribution of voids without velocity coherence. The angle θ is that subtended by the void pairwise velocity ($\Delta\vec{V}$) and the void relative separation ($\Delta\vec{R}$), as portrayed in panel (a). Panel (b) shows the results for all void pairs, panels (c) and (d) correspond to S-S and R-R pairs, respectively. Dotted lines represent the deciles of the distribution of cos(θ).

direction, showing that the void inner material and the surrounding haloes have a global common motion. We find that, for 90 per cent of the sample, the direction of the bulk motion of the inner mass in voids and the haloes in the surrounding shell agree within 20 degrees, differing in less than ~50 km s^{-1}in magnitude. In consequence, we argue that the use of haloes (or galaxies) in the shell is suitable to compute the void bulk velocity with the advantage of the significantly larger number of massive haloes and/or luminous galaxies than in the void core region. We notice that the magnitudes of void peculiar velocities (~300-400 km s^{-1}) are comparable to the mean velocity of the highest density peaks of the large scale structure, such as galaxy clusters. A more detailed study of the bulk motions of voids will be the subject of a forthcomming paper.

3.2 Coherence and bimodality of void relative motions

In this subsection we analyze whether void bulk motions are randomly distributed, or their dynamics is related to the large scale structure and in particular to the void distribution. With this aim we have analysed the pairwise relative velocities of voids in the simulation in order to explore the coherence of the velocity field traced by voids. We have calculated the number of voids in relative separation, $d = |\Delta\vec{R}|$, and cos(θ) bins, where θ is the angle between the void relative velocity and the void relative separation vectors. The geometry of this calculation is shown in panel (a) of Figure 2. Thus, when the members of a void pair are mutually approaching (receding), the cosine of the angle between the relative velocity $\Delta\vec{V} = \vec{V}_2 - \vec{V}_1$ and the relative position $\Delta\vec{R} = \vec{R}_2 - \vec{R}_1$ is negative (positive), while for a non coherent motion it is expected a uniform distribution of cos(θ). In panel (b) of Figure 2 we show the number counts of void pairs as a function of cos(θ) and separation. We normalize these number counts with the expectation from a uniform distribution of voids without velocity coherence. It can be clearly seen the presence of two peaks, particularly within void separations lesser than 200 h^{-1} Mpc , showing the presence of two populations with voids mutually receding and approaching.

We have analysed this somewhat unexpected result within the framework of the seminal work of Sheth & van de Weygaert (2004), who studied the evolution of cosmic voids in the context of a hierarchical scenario of structure formation. They introduced the so called void-in-void and void-in-cloud schemes, where voids are affected by the surrounding distribution of mass. This model agrees with the observed dynamics in SDSS voids (Paz et al. 2013): depending on their environment, some of the voids shrink while others are in expansion. Given this strong dichotomy of void dynamics, we have attempted at linking the void pairwise velocity coherence shown in panel (b) of Figure 2 to their local environment.

Following the methods described in Ceccarelli et al. (2013), we have defined voids with continuously rising integrated radial density profiles (R-type, a proxy for void-in-void), and void samples that exhibit an overdense shell (S-type, a proxy for void-in-cloud). By construction, these R- and S-type void samples exhibit different dynamical properties (Paz et al. 2013; Ruiz et al. 2015). Here, we further explore the possible connection between void types and the bimodality of the relative motions shown in panel (b) of Figure 2. Remarkably, the observed bimodal behavior can be completely understood in terms of the R/S void type classification. As it can be seen in panels (c) and (d), S-type void pairs are systematically approaching each other, and conversely R-type voids are mutually receding. We notice that the relative fraction of R/S void types depends on void radius (Ceccarelli et al. 2013), small voids are typically S-types while large voids are mainly R-type. Thus the prominence of the two peaks seen in this Figure, would vary according to the sample mix of void sizes. As expected, at

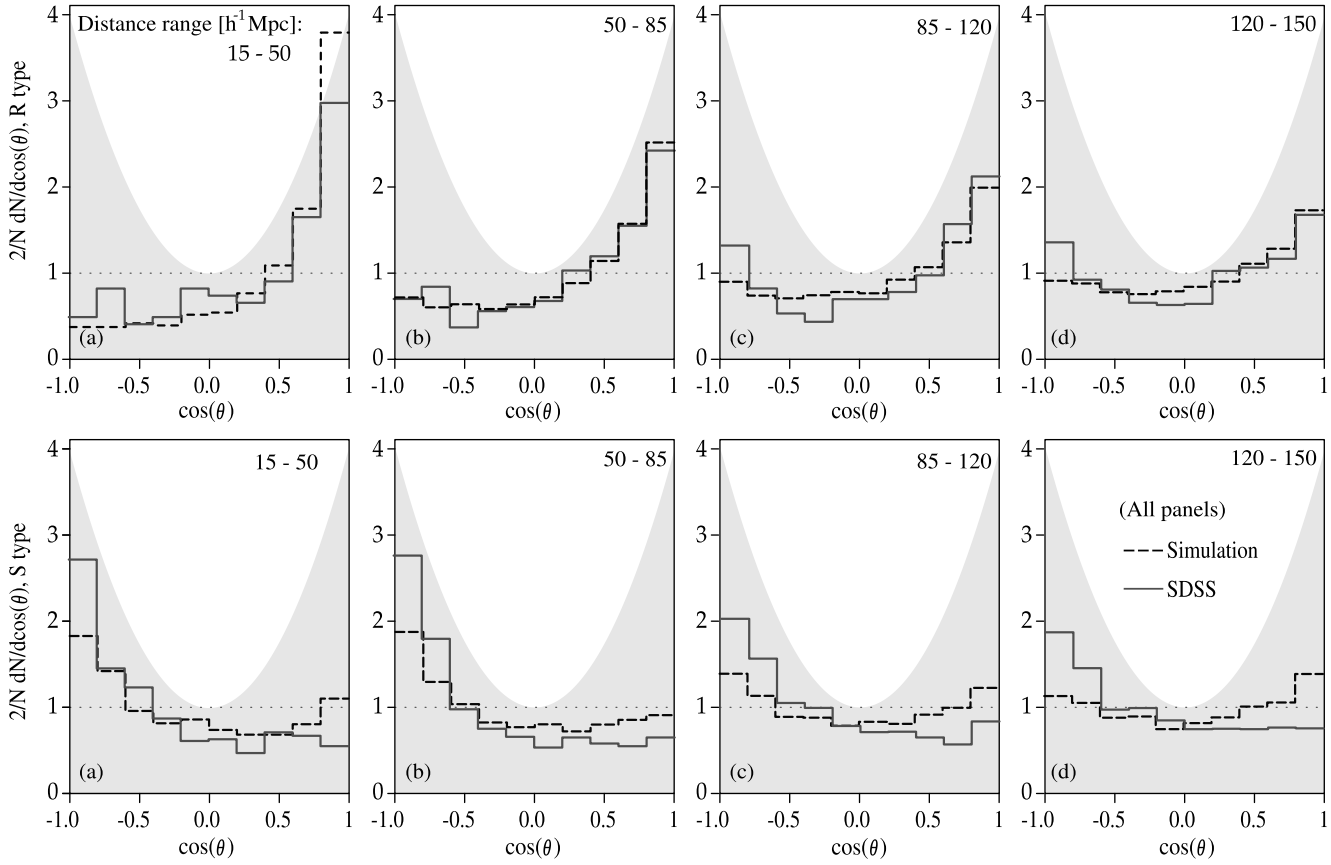

Figure 3. Bimodality of relative motions in the simulation and SDSS data. The histograms of cos(θ) correspond to void pair separations in the ranges 15-50 h^{-1} Mpc (panels a), 50-80 h^{-1} Mpc (panels b), 80-120 h^{-1} Mpc (panels c) and 120-150 h^{-1} Mpc (panels d). Upper (bottom) panels correspond to R-type (S-type) void pairs in the simulation box (dashed lines) and the observations (solid lines). We show for reference a quadrupolar distribution with arbitrary normalization. Histograms are normalized to show the excess of void pairs with respect to the expectation from a random distribution.

sufficiently large separations, the results are consistent with uncorrelated motions of void pairs.

In order to analyse this behaviour in the observations, we use void samples taken from the SDSS data together with the velocity field derived by Wang et al. (2012). Figure 3 shows the distribution of the cosine of the relative angle between the pairwise void velocity and the relative separation vector for both observational and simulated voids. As seen in this Figure, we also obtain a bimodal behavior for observational voids finding a very good agreement between observations and the simulation results. According to the environment classification of voids, there is a strong relative motion coherence which gently declines towards large separations. We also computed the pairwise velocities of haloes and the relative angles between pairs, finding that the motions of haloes also exhibit a bimodal behaviour. This indicates that the coherence pattern is not a peerless feature of voids, but a ubiquitous consecuence of the large scale distribution of matter. However, voids offer the oportunity to analyze this coherence pattern in its double regime of approaching and receeding systems according to their environment. We will further discuss these results in an upcoming paper.

In order to assess the magnitude of the coherent motions in the observed Universe, we show in Figure 4 the mean pairwise velocity values of the SDSS voids as a function of void relative separation, for R-R void pairs (filled squares) and S-S voids pairs (empty circles). The points correspond to the mean values of $V_{//} = |\Delta\vec{V}|\cos(\theta)$ and the error bars represent the uncertainties derived through Jackknife resampling of the void data. The colour density map correspond to the results of R-R and S-S void pairs in 500 different sub–boxes taken at random from the simulation constrained to have similar SDSS volumes and geometry, thus accounting for cosmic variance in the SDSS region. Blue (red) shaded areas correspond to the number density of curves for S-S (R-R) void pairs. The thin blue and red lines correspond to the 0.16 and 0.84 quantiles of the distribution of $V_{//}$, for S-S and R-R void pairs, respectively. The thick dashed lines correspond to the full simulation box results for R-R and S-S pairs. As it can be seen in this Figure, the observational results are entirely consistent with the prediction of the ΛCDM model. Voids behave either receding or approaching each other according to their R/S-type classification with velocities of the order of 100–150 km s^{-1} up to 200 h^{-1} Mpc separation.

4 DISCUSSION

At a first glance, the coherence and non-negligible motions of voids have important effects for observational cosmology. In particular, cosmological tests such as the Alcock-Paczynski (Lavaux & Wandelt 2010; Sutter et al. 2012) or the Integrated Sachs-Wolfe effect

(Granett et al. 2008; Pápai et al. 2011; Hernández-Monteagudo & Smith 2013; Ilić et al. 2013; Cai et al. 2014), depend on a proper modeling of the velocity and density fields surrounding voids. The existence of coherent void motions in large cosmological volumes can also impact on cosmological tests using voids in forthcoming large-scale surveys.

Aside the implications on cosmological parameter estimation, the motion of voids and its coherence, seen here by first time on observations and the concordance cosmology simulation, is itself important. These results could help to understand the formation and evolution of structure in the larger scales that have been studied so far. The magnitude of the velocities involved, around 400 km s^{-1}, and the coherence of such motions up to scales of 200 h^{-1} Mpc, is expected to drive the formation of future large scale structures in the Universe (Anderson et al. 2014). Another interesting implications of our results can be found in studies of the bulk flow motion of galaxies and clusters at large scales (Nusser et al. 2011; Turnbull et al. 2012; Ma & Pan 2014; Hoffman et al. 2015). The measurements of a non-negligible bulk flow at scales around a few 100 h^{-1} Mpc is source of tension between real data and the ΛCDM model. A large amplitude of bulk flow (e.g. ∼400 km s^{-1}) can be taken as an indication of the presence of significant density fluctuations at very large scales (Watkins et al. 2009). The existence of such fluctuations could be incompatible with cosmological models derived from Cosmic Microwave Background probes (Watkins et al. 2009; Lavaux et al. 2010; Feldman et al. 2010; Colin et al. 2011). Our results contribute to the field by adding a possible scenario for large scale flows based on the concordance cosmological model. The correlated mutual void velocities observed here can be conducing at some extent the motion of clusters and galaxies at intermediate densities, in filaments or walls.

Summarizing, this letter reports by first time on the significant motions of cosmic voids as a whole and study the coherence pattern associated to the void velocity field up to large cosmological scales, both in simulations and observations. By embracing the idea that voids are moving objects, our results have an important impact on future cosmological test planed for the next generation of large volume surveys. Void coherent bulk velocities, with a bimodal dynamical population of mutually attracting or receding systems, contribute to imprint large scale cosmic flows, shaping the formation of future structures in the Universe.

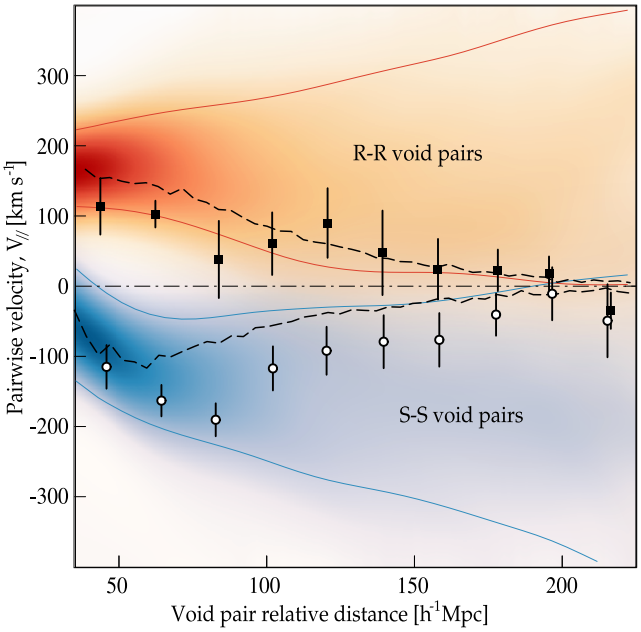

Figure 4. Void pairwise velocity ($V_{//}$) as a function of relative separation in the SDSS data and the simulation. Points represent SDSS values of $V_{//}$ and its uncertainty computed through Jackknife resampling. Dashed lines show the median values of $V_{//}$ in the full-box simulation. Red and blue regions represent the cosmic variance obtained from subsets of the simulation with similar volume and geometry than the SDSS survey for R- and S-types, respectively. The 0.16 and 0.84 quantiles of the distribution of $V_{//}$ values are shown in solid lines.

ACKNOWLEDGMENTS

This work was partially supported by the Consejo Nacional de Investigaciones Científicas y Técnicas (CONICET), and the Secretaría de Ciencia y Tecnología, Universidad Nacional de Córdoba, Argentina. We thank the anonymous referee for useful suggestions that significantly increase the correctness and quality of this work. We thank Dr. Mario A. Sgró for kindly providing the numerical simulation and halo catalogue. Plots are made using R software. This research has made use of NASA's Astrophysics Data System.

REFERENCES

Abazajian K. N., et al., 2009, ApJSS, 182, 543
Amendola L., et al., 2013, Living Reviews in Relativity, 16, 6
Anderson L., et al., 2014, MNRAS, 441, 24
Behroozi P. S., Wechsler R. H., Wu H.-Y., 2013, ApJ, 762, 109
Bos E. G. P., van de Weygaert R., Dolag K., Pettorino V., 2012, MNRAS, 426, 440
Branchini E., Davis M., Nusser A., 2012, MNRAS, 424, 472
Cai Y.-C., Neyrinck M. C., Szapudi I., Cole S., Frenk C. S., 2014, ApJ, 786, 110
Ceccarelli L., Padilla N. D., Valotto C., Lambas D. G., 2006, MNRAS, 373, 1440
Ceccarelli L., Padilla N., Lambas D. G., 2008, MNRAS, 390, L9
Ceccarelli L., Paz D., Lares M., Padilla N., Lambas D. G., 2013, MNRAS, 434, 1435
Colin J., Mohayaee R., Sarkar S., Shafieloo A., 2011, MNRAS, 414, 264
Einasto M., Tago E., Jaaniste J., Einasto J., Andernach H., 1997, A&AS, 123, 119
Einasto M., et al., 2012, A&A, 542, 36
Feldman H. A., Watkins R., Hudson M. J., 2010, MNRAS, 407, 2328
Frisch P., Einasto J., Einasto M., Freudling W., Fricke K. J., Gramann M., Saar V., Toomet O., 1995, A&A, 296, 611
Granett B. R., Neyrinck M. C., Szapudi I., 2008, ApJ, 683, L99
Hahn O., Abel T., 2011, MNRAS, 415, 2101
Hernández-Monteagudo C., Smith R. E., 2013, MNRAS, 435, 1094
Hill G. J., et al., 2008, in Kodama T., Yamada T., Aoki K., eds, Astronomical Society of the Pacific Conference Series Vol. 399, Panoramic Views of Galaxy Formation and Evolution. p. 115
Hinshaw G., et al., 2013, ApJS, 208, 19
Hoffman Y., Courtois H. M., Tully R. B., 2015, MNRAS, 449, 4494
Ilić S., Langer M., Douspis M., 2013, A&A, 556, A51
Lavaux G., Wandelt B. D., 2010, MNRAS, 403, 1392
Lavaux G., Tully R. B., Mohayaee R., Colombi S., 2010, ApJ, 709, 483
Ma Y.-Z., Pan J., 2014, MNRAS, 437, 1996
Nusser A., Branchini E., Davis M., 2011, ApJ, 735, 77
Padilla N. D., Ceccarelli L., Lambas D. G., 2005, MNRAS, 363, 977
Pápai P., Szapudi I., Granett B. R., 2011, ApJ, 732, 27
Paz D., Lares M., Ceccarelli L., Padilla N., Lambas D. G., 2013, MNRAS, 436, 3480

Ricciardelli E., Cava A., Varela J., Quilis V., 2014, MNRAS, 445, 4045
Ruiz A. N., Paz D. J., Lares M., Luparello H. E., Ceccarelli L., Lambas D. G., 2015, MNRAS, 448, 1471
Sheth R. K., van de Weygaert R., 2004, MNRAS, 350, 517
Springel V., 2005, MNRAS, 364, 1105
Sutter P. M., Lavaux G., Wandelt B. D., Weinberg D. H., 2012, ApJ, 761, 187
Turnbull S. J., Hudson M. J., Feldman H. A., Hicken M., Kirshner R. P., Watkins R., 2012, MNRAS, 420, 447
Wang H., Mo H. J., Jing Y. P., Guo Y., van den Bosch F. C., Yang X., 2009, MNRAS, 394, 398
Wang H., Mo H. J., Yang X., van den Bosch F. C., 2012, MNRAS, 420, 1809
Watkins R., Feldman H. A., Hudson M. J., 2009, MNRAS, 392, 743
van de Weygaert R., Bertschinger E., 1996, MNRAS, 281, 84

This paper has been typeset from a TEX/LATEX file prepared by the author.